

Physics Considerations in the Design of NCSX*

G. H. Neilson¹, M. C. Zarnstorff¹, L. P. Ku¹, E. A. Lazarus², P. K. Mioduszewski²,
 W. A. Cooper³, M. Fenstermacher⁴, E. Fredrickson¹, G. Y. Fu¹, A. Grossman⁵,
 P. J. Heitzenroeder¹, R. H. Hatcher¹, S. P. Hirshman², S. R. Hudson¹, M. Isaev⁶,
 D. W. Johnson¹, H. W. Kugel¹, J. F. Lyon², R. Majeski¹, M. Mikhailov⁶, D. R. Mikkelsen¹,
 D. A. Monticello¹, H. E. Mynick¹, B. E. Nelson², N. Pomphrey¹, W. T. Reiersen¹,
 A. H. Reiman¹, P. H. Rutherford¹, J. A. Schmidt¹, D. A. Spong², D. J. Strickler², A. Subbotin⁶

- 1) Princeton Plasma Physics Laboratory, Princeton, NJ 08543
- 2) Oak Ridge National Laboratory, Oak Ridge, TN 37831
- 3) École Polytechnique Federale de Lausanne, Lausanne, Switzerland.
- 4) Lawrence Livermore National Laboratory, Livermore, CA 94550.
- 5) University of California at San Diego, San Diego, CA 92093.
- 6) RRC Kurchatov Institute, Moscow, Russia.

e-mail contact of main author: hneilson@pppl.gov

Abstract. Compact stellarators have the potential to make steady-state, disruption-free magnetic fusion systems with $\beta \sim 5\%$ and relatively low aspect ratio ($R/\langle a \rangle < 4.5$) compared to most drift-optimized stellarators. Magnetic quasi-symmetry can be used to reduce orbit losses. The National Compact Stellarator Experiment (NCSX) is designed to test compact stellarator physics in a high-beta quasi-axisymmetric configuration and to determine the conditions for high-beta disruption-free operation. It is designed around a reference plasma with low ripple, good magnetic surfaces, and stability to the important ideal instabilities at $\beta \sim 4\%$. The device size, available heating power, and pulse lengths provide access to a high-beta target plasma state. The NCSX has magnetic flexibility to explore a wide range of equilibrium conditions and has operational flexibility to achieve a wide range of beta and collisionality values. The design provides space to accommodate plasma-facing components for divertor operation and ports for an extensive array of diagnostics.

1. Introduction

Fusion energy research is increasingly focused on the challenge of finding the best magnetic configuration for a practical fusion reactor. Stellarators are of particular interest because they can solve two major problems for magnetic confinement— achieving steady state operation and avoiding disruptions. Consequently, substantial investments are being made in new stellarator facilities, including the large superconducting LHD [1] and W7-X [2] experiments. The three-dimensional plasma geometry of stellarators provides degrees of freedom, not available in axisymmetric configurations, to target favorable physics properties (low magnetic field ripple, well-confined particle orbits, high-beta stability without the need for current drive or feedback) in their design. Design features now being studied experimentally include the use of helical magnetic-axis excursions (TJ-II [3], H1-NF [4], and Heliotron-J [5]) and approximate alignment of particle drift orbits with magnetic surfaces (W7-AS [6] and W7-X [2]).

In quasi-symmetric stellarator design the 3D magnetic field strength has an approximate symmetry direction in Boozer coordinates [7] to keep charged particle drift orbits well confined. Compact stellarators are designed with an aspect ratio $R/\langle a \rangle$ much less than that of

* Research supported by the U.S. Department of Energy under Contract No. DE-AC76-CH0-3073 with the Princeton Plasma Physics Laboratory and Contract No. DE-AC05-00OR-22725 with the Oak Ridge National Laboratory.

currentless optimized stellarators (≤ 4.5 vs. ≥ 10). Stellarator coils are designed to generate most of the rotational transform and to shape the plasma to achieve the desired physics properties. The bootstrap current can be used to generate some of the rotational transform (iota). Care must be taken in the design to minimize islands which are a feature of the three-dimensional geometry.

The National Compact Stellarator Experiment (NCSX) [8, 9] is designed to be a quasi-axisymmetric stellarator (QAS), so that its transport properties are similar to those of tokamaks. The design has high beta ($> 4\%$), moderate aspect ratio (≤ 4.4), and “reversed” magnetic shear. A successful experimental test of magnetic quasi-symmetry has already been carried out in the Helically Symmetric Experiment (HSX) [10]. The mission of NCSX is to test compact stellarator physics in a high-beta QAS configuration and to determine the conditions for high-beta disruption-free operation in order to evaluate its potential as a fusion concept. A QAS strategy is also used in the CHS-qa study [11]. A quasi-poloidal, compact stellarator with lower aspect ratio is being designed for the QPS experiment [12].

2. Coil Design

The NCSX uses modular coils (Fig. 1) to generate the main helical magnetic field. For equilibrium flexibility, there are also toroidal field coils, poloidal field coils, and helical-field trim coils. The physics basis for the coil design is a computed three-period reference QAS plasma with $\beta = 4\%$. An assumed moderately broad pressure profile typical of experiments and a consistent bootstrap current profile which generates about one-fourth of the rotational transform at the edge are used.

Existing stellarator coil design methods, based on the VMEC [13] equilibrium code, were extended in order to design feasible coils and plasmas for low-aspect-ratio stellarators with internal currents. An initial filamentary

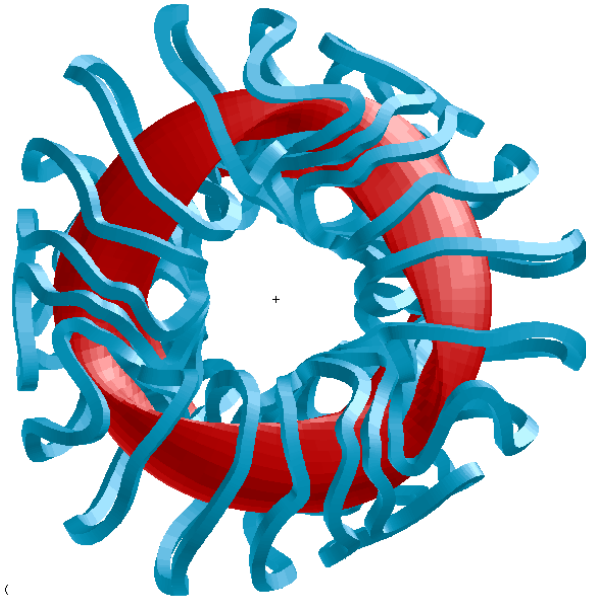


FIG. 1. NCSX modular coils and reference plasma.

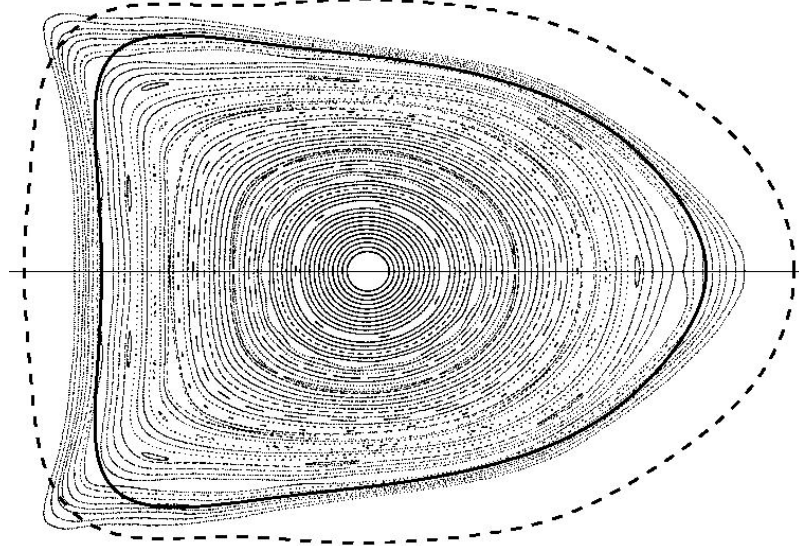


FIG. 2. Poincaré plots of PIES magnetic surfaces for target free-boundary PIES equilibrium at $\beta=4.1\%$ for finite-cross section model of NCSX coils. Dashed line: first wall; solid line: VMEC equilibrium boundary.

TABLE I. NCSX Configuration Physics Design Summary

Parameter or Property	Achieved in $\beta = 4\%$ Target Equilibrium	Criteria
Aspect ratio $R/\langle a \rangle$	4.4	Substantially lower than existing drift-optimized stellarator designs, e.g. HSX, W7-X.
Stability at $\langle \beta \rangle = 4\%$	Stable to ext. kink, vertical, Mercier modes	Sufficient to test stabilization of a sustainable toroidal plasma by 3D shaping.
Shear	$\iota = 0.39$ (center), 0.65 (edge)	For neoclassical island reduction and healing. Monotonically increasing except very near the edge.
Large external ι fraction.	~ 0.75 from coils	Conservative approach for disruption-resistance.
Quasi-symmetry	effective ripple $\varepsilon_h \approx 0.1\%$ (center), 0.4% ($r/a \approx 0.7$).	Low helical ripple neoclassical transport compared to axisymmetric designs; tolerable balanced neutral-beam-injected ion losses in high-beta, low-B scenarios.
Magnetic surface quality	total effective island width $< 10\%$ of toroidal flux	For negligible contribution to losses. Based on PIES equilibrium calculations and estimated neoclassical and finite- $\chi_\perp/\chi_\parallel$ island width corrections.

modular coil solution is found by minimizing the root-mean-squared normal component of the magnetic field on the surface of the reference plasma, following the “reverse engineering” approach used in the W7-X design [14]. The coil geometry is then modified by a technique which couples the coil [15] and plasma optimization processes to directly design coils which produce a free-boundary target equilibrium possessing the reference plasma physics properties (rather than a particular shape), as well as engineering parameters such as coil spacing and bend radius. The achieved physics properties are summarized in Table I. An effective ripple parameter ε_h , characterizing transport in the $1/\nu$ regime [16], measures the degree of quasi-axisymmetry. In the final step, the coil geometry is modified again using a technique to reduce the width of residual islands in the free-boundary equilibrium calculated by the PIES code [17]. The coil design process leads to a free-boundary high-beta target equilibrium that has good magnetic surfaces, with the sum of effective island widths $< 1\%$ with finite-model coils (Fig. 2), while preserving target physics and engineering properties.

Although optimized for a single equilibrium, the NCSX coil design can support a broad range of equilibria with favorable physics properties and a wide range of plasma profiles, as is necessary for its mission. This is accomplished by varying the currents in the toroidal field, poloidal field, and modular coil circuits. Since it is planned to initiate NCSX plasmas on vacuum magnetic surfaces, the existence of good vacuum configurations is critical. A vacuum case with $\iota < 0.5$ everywhere, is shown in Fig. 3. Good configurations with $\iota > 0.5$ are also available, providing flexibility to either encounter or avoid possible instabilities associated with the $\iota = 0.5$ resonance during startup.

The coil design provides a wide operating space in β and plasma current (I_p) for the reference pressure and current profile shapes and constant magnetic field ($B = 1.7$ T at $R = 1.4$ m). As shown in Fig. 4, VMEC equilibria stable to external kink and ballooning modes and having low ripple ϵ_h can be made with β ranging from 0 to 4% and I_p from 0 to 100% of its reference value. Stable equilibria at higher beta (at least 6%) can be made with modest increase in ripple. The design is robust to variations in pressure and current profile shapes. While the reference current profile is hollow, stable equilibria with $\beta = 3\%$, and $\epsilon_h < 0.5\%$ are found with peaked current profiles as well.

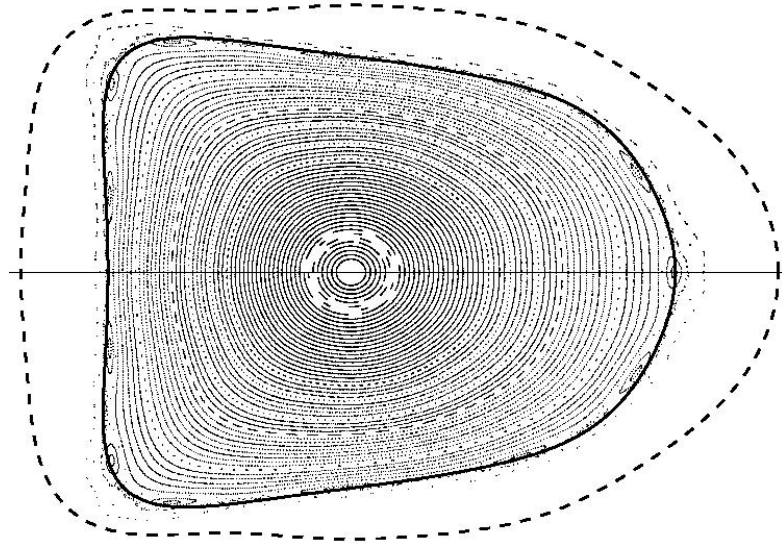


FIG. 3. Poincaré plots of PIES magnetic surfaces for vacuum configuration with iota of 0.43-0.46 (filamentary coil model). Dashed line: first wall; solid line: VMEC equilibrium boundary.

By varying coil currents, the equilibrium parameters to which the physics properties are sensitive can be varied, providing the capability to test theoretical predictions. Kink stability beta limits can be lowered from the nominal 4% to about 1% so theoretical stability limits can be studied over a range of beta values. While the design has been optimized to make the effective ripple at $r/a \approx 0.7$ very low, it can easily be increased by almost an order of magnitude, while preserving stability, to test the dependence of neoclassical losses and confinement enhancement on the degree of quasi-symmetry. The rotational transform profile can be varied to study its effects on transport and stability. The external rotational transform can be varied at fixed shear from -0.2 to $+0.1$ about the reference profile. The global shear ($\iota_{\text{edge}} - \iota_0$) can be increased by a factor of 2 at fixed ι_0 ; limits on reducing the shear are still being studied.

Satisfactory magnetic surfaces have been calculated with PIES for several points in the NCSX

		Beta (%)						
		0	1	2	3	4	5	6
Current (kA)	0	0.82%	0.89%	0.79%				
	44	0.77%	0.68%	0.67%	0.61%	0.72%		
	88	0.71%	0.65%	0.51%	0.72%	0.60%		
	131	0.52%	0.46%	0.42%	0.41%	0.45%		
	174	0.37%	0.39%	0.36%	0.40%	0.45%	0.92%	
	200							

FIG. 4. Operating diagram in plasma current-beta space for NCSX coils and reference profiles. Effective ripple (ϵ_h) at $r/a \approx 0.7$ are identified for equilibria found stable to external kink and ballooning modes. Shaded equilibria are unstable. Unmarked regions were not analyzed.

operating space, but additional island width control may be needed. Planned resonant trim coils can be added to provide additional control of island-producing resonances for purposes of reducing island widths or performing controlled island physics experiments.

3. Device Size and Performance

The NCSX device size (major radius $R = 1.4$ m), magnetic field range ($B = 1.2$ - 2.0 Tesla), pulse length (0.3-1.2 s) and plasma heating power (initially 3 MW) are set to produce the plasma conditions and profiles needed to test critical physics issues over a range of beta and collisionality values. The device will be initially equipped with two of the four existing 1.5-MW, 50-keV, 0.3-s neutral beam injectors, formerly used on the PBX-M experiment. They are arranged for balanced tangential injection to be able to balance rotational transform perturbations due to beam-driven currents. Monte Carlo beam slowing down calculations predict 24% hydrogen beam ion loss for balanced injection at $B = 1.2$ T. Plasmas with $\beta = 2.6\%$ and collisionality $\nu^* = 0.25$ are predicted with the initial 3-MW beam system, assuming an enhancement factor of 2.9 times the ISS95 [18] stellarator confinement time scaling, or 0.9 times an equivalent ITER-97P L-mode tokamak scaling [19]. With the full complement of hydrogen neutral beams (6 MW) and these same confinement enhancement assumptions, the reference beta value of 4% and collisionality $\nu^* = 0.25$ predicted. The ISS95 enhancement factor required to reach 4% beta is reduced to 1.8 by allowing the density to rise to the Sudo limit [20], with an attendant increase in collisionality.

The NCSX magnet system is designed for pulsed operating scenarios with magnetic fields up to 2.0 T (for 0.2 s) for low-collisionality plasma studies and pulse lengths up to 1.2 s (at $B = 1.2$ T) for experiments with pulse lengths long compared to current equilibration times. The magnet design also provides operating scenarios with plasma current up to 350 kA (providing a factor of 2 range for internal rotational transform flexibility). The neutral beam pulse length can be increased to 0.5 s with modest changes and potentially to >1 s with additional upgrades. Radio frequency waves can be launched from the high-field side to more directly heat electrons than with the neutral beams.

4. Discharge Evolution

Time-dependent modeling of NCSX discharge evolution has been carried out to demonstrate the existence of satisfactory paths from vacuum fields to a target high-beta state, consistent with the technical capabilities of the coils and heating systems. The coils are designed to provide Ohmic heating, current drive, external rotational transform, and plasma shape control. Neutral beams provide plasma heating and current drive, although the balance of co- and counter-injection is adjusted to minimize the latter. The bootstrap current provides significant rotational transform.

A simulation methodology based on the TRANSP 1-1/2-D tokamak analysis code was developed to model the time-evolution of the poloidal flux and iota profile. Because NCSX is quasi-axisymmetric, tokamak modeling tools can provide an accurate guide. An equivalent tokamak equilibrium is generated having the same external iota, major radius, aspect ratio, plasma volume, and toroidal flux as the reference NCSX equilibrium. In the simulation, the plasma shape, external iota profile (simulated as an externally-specified driven current profile), and density profile shape are kept constant in time. The plasma current, density, neutral beam heating power, and co-/counter- beam balance are programmed. The electron and ion thermal diffusivities are automatically adjusted to match an assumed global energy

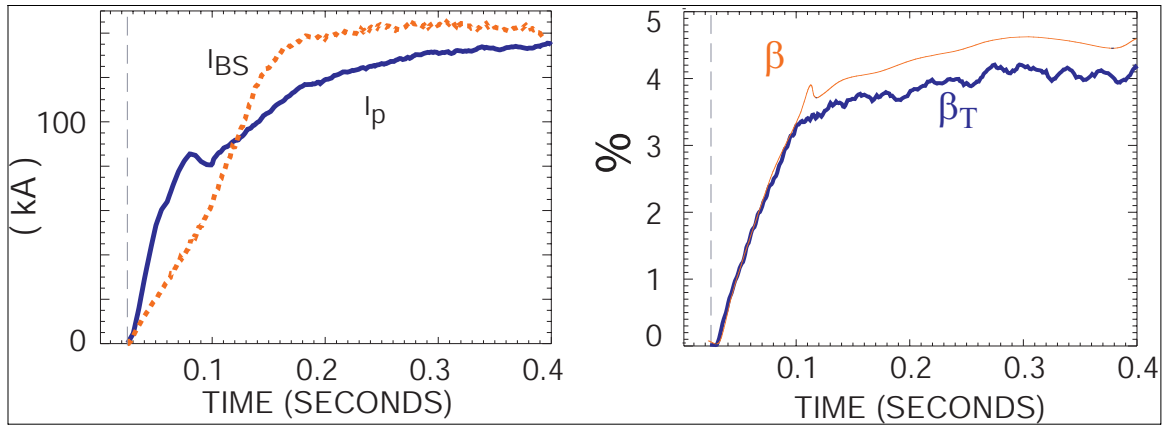


FIG. 5. Waveforms from time-dependent simulation of high-beta NCSX discharge. (a) Plasma current (programmed) and calculated bootstrap current. (b) Calculated beta values using tokamak (β_T) and stellarator (β) definitions.

confinement scaling (minimum of neo-Alcator and ITER-97P L-mode scaling). The TRANSP code models poloidal flux diffusion, beam deposition and slowing down, neutral beam current drive, and power balance. It calculates the profiles of electron and ion temperature and pressure, fast ion pressure, current, and iota. The transformation to the actual NCSX geometry is accomplished by using the VMEC code to calculate a time-series of free-boundary equilibria with the actual NCSX coil geometry and the TRANSP-simulated profiles as input.

Results are presented here for a simulation with $B = 1.4$ T and an available 6 MW of balanced neutral beam injection. Figure 5 shows time sequences of key input and output parameters of the 1-1/2-D modeling. Important aspects of discharge programming to obtain the target beta and a nearly stationary bootstrap current profile at the end of the discharge are minimizing the Ohmic current during startup, adjusting the co-counter beam balance to approximately balance the Ohmic current profile, rapidly (~ 1.5 MA/s) increasing the current initially followed by clamping of the applied loop voltage, and modulating the neutral beam heating power to control the total pressure. At $t = 303$ ms of the TRANSP simulation, the average toroidal beta has risen to about 4% (corresponding to 4.5% when transformed to a stellarator equilibrium because of a different magnetic field normalization), peak electron and ion temperatures are 2.4 keV and 2.8 keV respectively, and the volume-averaged electron and ion collisionality values are $\nu_e^* = 0.2$, $\nu_i^* = 0.1$. The current (130 kA) is well matched to the bootstrap current (140 kA), and the current profile is predominantly bootstrap. The parameters and profiles in this state are similar, though not identical, to those of the reference equil-

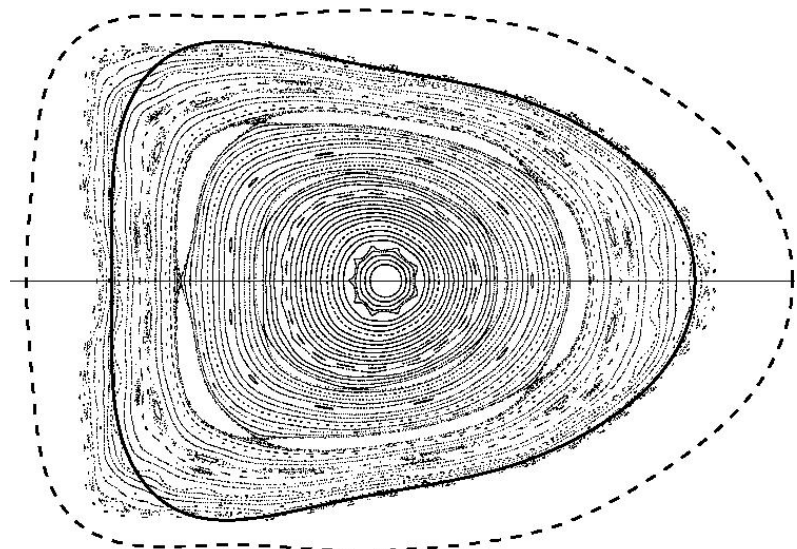


FIG. 6. Poincaré plots of PIES magnetic surfaces for equilibrium at $t = 303$ ms in discharge simulation. Dashed line: first wall; solid line: VMEC equilibrium boundary.

ilibrium. Free-boundary VMEC equilibria were generated for the sequence of profiles resulting from this simulation and the NCSX coils by varying the coil currents to optimize physics properties. The plasma is calculated to be stable to ballooning, kink, and vertical modes and to have good quasi-axisymmetry ($\epsilon_h < 0.4\%$ at $r/a \approx 0.5$) throughout the discharge.

Magnetic surface quality is analyzed using the PIES code. Results at $t = 303$ ms, when 99% of the current is bootstrap, are shown in Fig. 6. The $m = 5$ island, which extends over 5% of the cross-section area in the PIES calculation, is predicted to be reduced to 2.5% by neoclassical effects which are not included in the PIES calculations. The island widths can also be reduced using the trim coils. A number of small island chains are visible in Figure 5. When the island width is smaller than a critical value, electron diffusion across the island dominates diffusion along the field line, and the presence of the island has little effect on transport. The critical island width is about 2%-3% of the minor radius for the mode numbers of interest.

5. Power and Particle Handling

Control of impurities and neutral recycling is the main power and particle handling issue in the design of NCSX. [21] For impurity control, low-Z materials (carbon) are planned for surfaces with intense plasma-wall interactions. For neutral control, recycling sources and baffles will be arranged so as to inhibit neutral flow to the main plasma. Motivated in part by recent W7-AS divertor results showing improved edge control and plasma performance [22], the NCSX is designed so that a pumped slot divertor can be installed in the future. The basic requirement affecting the design of the coils and the vacuum vessel is providing sufficient connection length of field lines in the scrapeoff layer outside the last closed magnetic surface (LCMS). Connection lengths longer than 100 m are sufficient to allow high temperatures at the LCMS and significant temperature drops along field lines to reasonably low target temperatures, and hence the establishment of low temperatures and a high recycling regime to control the impurity source at the target.

Scrapeoff layer field-line following calculations for magnetic configurations which have finite plasma pressure were made using the MFBE code [23]. In NCSX the field lines launched close to the LCMS (here taken to be the VMEC boundary) make many toroidal revolutions close to it and do not exhibit very strong stochasticity. This is seen in Fig. 7, a Poincaré plot of scrapeoff field lines for the reference high-beta state and the NCSX coils. The field lines are launched from the midplane, half from the inside and half from the outside, from 0 to 10 mm outside the LCMS. Most lines remain within a 4-cm wide band conformal to the boundary (except near the tips of the banana-shaped cross sections, where the divertor would be located) long enough to complete 20 toroidal revolutions (~ 200 m) and provide the required connection lengths. These calculations are used as

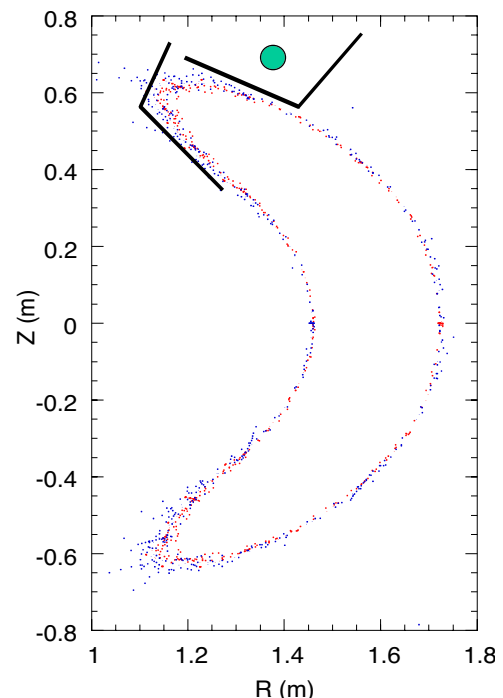


FIG. 7 Poincaré plots of scrapeoff field lines started at the inboard and outboard midplane within 0-1 cm of the nominal (VMEC) boundary and followed for 20 toroidal revolutions. Envisioned divertor hardware is indicated schematically.

a guide in the placement of plasma-facing components with sufficient clearance to provide long connection lengths.

6. Summary

The NCSX is designed to provide the capabilities needed to assess the physics of compact stellarators. It will produce high beta equilibria with good physics properties and magnetic surfaces, have an ample operating space and flexibility, and provide access to high-beta target equilibria starting from vacuum. Based on these physics considerations, a feasible engineering concept for the NCSX has been developed. [24] It provides the space and access provisions to augment the initial configuration with new capabilities, particularly diagnostics [25] and plasma-facing components, as needed in the course of the experimental program.

-
- [1] FUJIWARA, M., et al., in Fusion Energy 2000 (Proc. 18th Conf., Sorrento, Italy, 4-10 Oct., 2000), IAEA, Vienna (2001), Paper IAEA-CN-77-OV1/4.
 - [2] LOTZ, W., et al., in Plasma Physics and Controlled Nuclear Fusion Research 1990 (Proc. 13th Int. Conf. Washington, 1990) Vol.2, IAEA, Vienna (1991) 603.
 - [3] ALEJALDRE, C., et al., in Fusion Energy 2000 (Proc. 18th Conf., Sorrento, Italy, 4-10 Oct., 2000), IAEA, Vienna (2001), Paper IAEA-CN-77-OV4/4.
 - [4] HARRIS, J. H., et al., in Fusion Energy 2000 (Proc. 18th Conf., Sorrento, Italy, 4-10 Oct., 2000), IAEA, Vienna (2001), Paper IAEA-CN-77-EXP1/02.
 - [5] OBIKI, T., et al., in Fusion Energy 2000 (Proc. 18th Conf., Sorrento, Italy, 4-10 Oct., 2000), IAEA, Vienna (2001), Paper IAEA-CN-77-EXP1/09.
 - [6] SAPPER, J. et al., Fusion Technol. **17** (1990) 62.
 - [7] BOOZER, A. H., Phys. Fluids **23** (1980) 904.
 - [8] ZARNSTORFF, M., et al., in Fusion Energy 2000 (Proc. 18th Conf., Sorrento, Italy, 4-10 Oct., 2000), IAEA, Vienna (2001), Paper IAEA-CN-77-IC/1.
 - [9] NEILSON, G. H., et al., Phys. Plasmas **7** (2000) 1911.
 - [10] TALMADGE, J. N., this conference, Paper IAEA-CN-94-EX/P3-22.
 - [11] OKAMURA, S., et al., in Fusion Energy 2000 (Proc. 18th Conf., Sorrento, Italy, 4-10 Oct., 2000), IAEA, Vienna (2001), Paper IAEA-CN-77-ICP/16.
 - [12] SPONG, D. A., et al., Nucl. Fusion **41** (2001) 711; LYON, J. F., et al., this conference, Paper IAEA-CN-94-IC/P-05.
 - [13] HIRSHMAN, S. P., et al., Comput. Phys. Commun. **43** (1986) 143.
 - [14] NÜHRENBERG, J. and ZILLE, R., Phys. Lett. A **129** (1988) 113.
 - [15] STRICKLER D. J., et al., Fusion Sci. and Technol. **41** (2002) 107.
 - [16] NEMOV, V V., et al., Phys. Plasmas **6** (1999) 4622.
 - [17] HUDSON, S. R., et al., "Eliminating Islands in High-Pressure Free-Boundary Stellarator Magnetohydrodynamic Equilibrium Solutions," submitted to Phys. Rev. Lett.
 - [18] STROTH, U., et al., Nuclear Fusion **36** (1996) 1063.
 - [19] KAYE, S., et al., Nuclear Fusion **39** (1999) 1245.
 - [20] SUDO, S., et al., Nuclear Fusion **30** (1990) 11.
 - [21] MIODUSZEWSKI, P., et al., "Plasma boundary considerations for the National Compact Stellarator Experiment," Proceedings of 15th PSI Conference, Gifu, Japan, May 27-31, 2002, to be published in J. Nucl. Mat.
 - [22] GRIGULL, P. et al., 28th EPS Conference, Madeira, Portugal, 18-22 June, 2001
 - [23] STRUMBERGER, E. et al., Nucl Fusion, **37** (1997) 19.
 - [24] NELSON, B. E., et al., this conference, Paper IAEA-CN-94-FT/2-4.
 - [25] JOHNSON, D., et al., "Diagnostics Plan for the National Compact Stellarator Experiment," Rev. Sci. Inst., to be published.